JACS
JOURNAL OF THE AMERICAN CHEMICAL SOCIETY
pubs.acs.org/JACS
Article

Structural Mechanism for Gas Permeability in Noncrystalline Carbon under Pressure

Zhidan Zeng,*,# Hongbo Lou,# Fujun Lan, Xiao Sun, Yuxin Liu, Hongwei Sheng, Ho-kwang Mao, and Qiaoshi Zeng*

Cite This: https://doi.org/10.1021/jacs.5c17051

Read Online

ACCESS | Metrics & More | Article Recommendations | Supporting Information

ABSTRACT: Volatiles can form novel compounds and exhibit extraordinary properties under high pressure. The recently developed nanostructured diamond capsules (NDCs) enable the preservation of otherwise typically unquenchable high-pressure volatiles for fundamental research and practical applications in ambient environments. A critical process in NDC synthesis is the pressure-driven diffusion of volatiles into the enclosed nanopores of glassy carbon, the precursor material. However, the structural pathways that allow such diffusion remain unclear, as glassy carbon is typically considered to be extremely impermeable. Here, we combined in situ high-pressure synchrotron X-ray diffraction and small-angle X-ray scattering, complemented by transmission electron microscopy, to investigate the pressure-induced diffusion of two model gases, helium and argon, into glassy carbon and amorphous carbon. Our findings reveal that gas penetration occurs through disordered structural defects in glassy carbon rather than via the usually expected interlayer spacing between its weakly bonded graphene-like layers. Based on this mechanism, we further demonstrate that moderate pressures can also drive gas diffusion into various amorphous carbon nanospheres, identifying them as viable alternative precursors for NDCs. These findings close a critical gap in understanding gas permeability in disordered carbon under pressure and provide essential guidance for tailoring carbon precursors to optimize NDCs for applications with high-pressure volatiles.

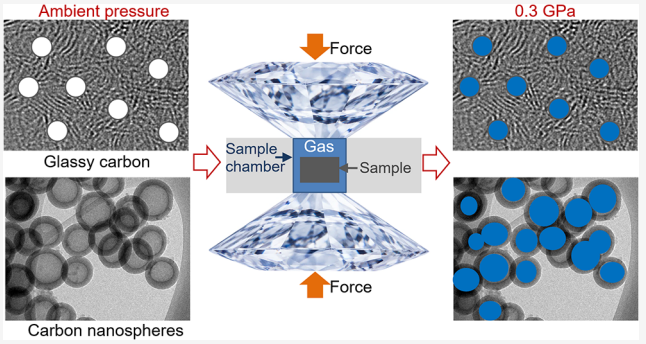

INTRODUCTION

Volatiles form exotic compounds and exhibit remarkable properties under high pressure, such as Xe−H_2, N_2−H_2, He−F compounds, near-room-temperature superconductivity in hydrogen sulfide, metallic hydrogen, and high-energy-density polymeric nitrogen.[1−8] However, these phenomena typically require sustained high-pressure conditions and are otherwise reversible upon decompression. Traditional high-pressure devices, such as large volume presses or diamond anvil cells (DACs), can generate and maintain a stable high-pressure environment for various materials, including volatiles. Unfortunately, these devices are incompatible with powerful but low-penetrating diagnostic probes like electron beams used in electron microscopy.[9] Additionally, their bulky nature restricts the practical applications of high-pressure volatiles at ambient conditions.[10] Recently, nanostructured diamond capsules (NDCs) have been developed as a solution,[11,12] enabling free-standing high-pressure volatile samples without relying on conventional high-pressure devices.

To synthesize NDCs, type 1 glassy carbon (GC) was used as a precursor (in the following text, GC refers to type 1 GC unless otherwise stated). GC is a bulk noncrystalline carbon with mostly sp^2 bonds and a layered structure consisting of randomly distributed curved graphene-like fragments.[13−15] Its structure and properties under high pressure have been extensively studied.[16−21] GC is synthesized through the pyrolysis of organic polymers at high temperatures; therefore, it contains numerous enclosed nanopores.[22] In the NDC synthesis process, a volatile substance, such as argon (Ar), is loaded into the sample chamber of a DAC along with GC. Upon compression, Ar diffuses into and fills the nanopores of the GC. Subsequent high-pressure, high-temperature treatment converts GC into diamond, forming NDCs containing high-pressure volatiles inside nanopores.[11] A key step in this process is pressurizing Ar into the nanopores of the GC, which act as high-pressure capsules. While GC is well-known for its excellent impermeability to gases (~10^9 cm^2/s) at ambient conditions, interestingly, high pressure is found to be able to significantly increase its permeability.[11] This allows volatiles

Received: September 27, 2025
Revised: December 24, 2025
Accepted: December 26, 2025

https://doi.org/10.1021/jacs.5c17051
J. Am. Chem. Soc. XXXX, XXX, XXX−XXX

such as Ar and neon (Ne) to diffuse into the enclosed nanopores of GC, enabling the successful synthesis of NDCs containing high-pressure Ar and Ne.

Despite the successful synthesis of NDCs containing high-pressure Ar and Ne, the mechanism of volatile diffusion in GC under high pressures remains unclear. Similar pressure-induced diffusion of helium (He) has been observed in silica glass,[23,24] which, like GC, is highly impermeable to gases or liquids under ambient conditions. It has been suggested that He might enter 6- and larger (7- and 8-)membered rings in silica due to its kinetic diameter (0.26 nm) being smaller than the size of interstitial sites in 6-membered rings (0.30 nm).[24] Given that graphene-like layers of GC also contain a significant number of 6-membered rings, along with some 7-membered rings, these structures may play a role in volatile diffusion. However, studies on graphene indicate that defect-free, single-layer graphene is nearly impermeable to all gases and liquids, including helium, neon, nitrogen, oxygen, and argon, up to 3 bar.[25,26] This suggests that volatiles likely cannot diffuse through 6-membered carbon rings in GC. On the other hand, unlike the network structure of silica glass, GC features a layered structure with a relatively large interlayer spacing of about 0.37 nm with weak van der Waals bonding,[27] which may serve as a diffusion pathway. A deeper understanding of the volatile diffusion mechanism and pathways in GC could guide the synthesis of NDCs containing other target high-pressure volatiles. Although GC has proven to be an effective precursor for NDC synthesis, identifying alternative carbon precursors with different atomic and microstructural characteristics is essential for broadening the synthesis and applications of NDCs. Understanding the mechanism of gas permeability in carbon could enable rational selection and design of new carbon precursors for NDC synthesis. However, no experimental studies have been conducted to date.

In this study, we combined in situ high-pressure synchrotron X-ray diffraction (XRD), high-pressure small-angle X-ray scattering (SAXS), and transmission electron microscopy (TEM) to investigate the diffusion of gas into GC and amorphous carbon under pressure. Our findings indicate that He does not diffuse into GC through the interlayer spacing between the graphene-like layers but rather through structural defects. As a consequence, pressure-induced permeability could be a general phenomenon in sp^2-bonded disordered carbon structures, not limited to GC. These results enhance our fundamental understanding of the permeability of disordered carbon under pressure and provide essential guidance for synthesizing various NDCs.

RESULTS AND DISCUSSION

Figure 1a compares the SAXS data of a GC sample at 0 GPa (without He) and those collected at 1.3 and 3.2 GPa with He. SAXS is an effective method for probing nanoscale density variations within materials. At 0 GPa, the SAXS profile shows a broad scattering peak at approximately 0.1−0.2 $Å^{-1}$, consistent with the presence of numerous nanopores in the GC, as previously reported.[11] A comparison of the experimental data and the modeling results using Irena software is shown in Figure S1.[28] The modeling decomposes the total signal into scattering from nanopores in GC and Porod-type background from large-scale structures (e.g., diamond anvils, beamline optics, and large domains in the sample). The irregular scattering peak at ∼0.02 $Å^{-1}$ originates from the scattering signal (Kossel line) from single-crystalline diamond anvils of

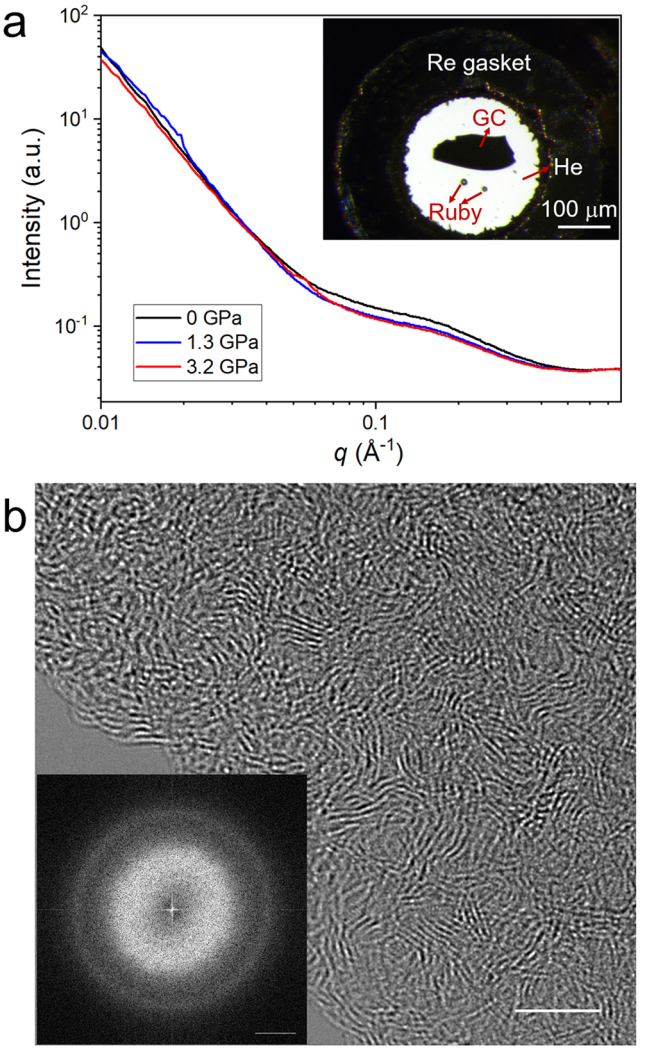

Figure 1. (a). SAXS curves of a GC sample in a DAC at 1.3 (blue), 3.2 (red), and 0 GPa (black curve) with He as the pressure-transmitting medium. The o GPa data was collected after decompression. Inset: the microscope image of the GC sample in the DAC for an in situ high-pressure SAXS experiment. (b) High-resolution TEM image of a GC sample showing the curved layer structure. The scale bar is 5 nm. Inset: the fast Fourier transform of the HRTEM image.

DAC.[29,30] Because the position and intensity of these Kossel line features vary with even subtle pressure-induced changes in the anvil orientation and strain, their appearance is pressure-dependent. At 1.3 GPa, the Kossel lines overlap with the sample-scattering region and could not be fully masked without significantly degrading the signal-to-noise ratio. At 1.3 GPa, with He present, the scattering peak (0.1−0.2 $Å^{-1}$) becomes obviously weaker. This change could be partly attributed to the diffusion of He into the nanopores, which reduces the density contrast between the GC matrix and the pores, and partly to the decreased pore volume due to compression.

A further increase in pressure to 3.2 GPa (a pressure increase of 1.9 GPa) results in only a subtle decrease in the intensity of the SAXS peak, suggesting a minor change in the pore volume. In contrast, previous studies suggest the volume of a GC sample decreases almost linearly during compression up to ∼11.2 GPa.[31] Therefore, the SAXS results imply that He

https://doi.org/10.1021/jacs.5c17051
J. Am. Chem. Soc. XXXX, XXX, XXX−XXX

is present in the nanopores, making them less compressible than empty pores. The ability of He to diffuse into GC aligns with previous experimental observations that inert gases Ne and Ar, which have larger kinetic diameters than He, can diffuse into GC under pressure.[11]

The next question is how He diffuses into GC under pressure. As shown in Figure 1b, GC consists of curved graphene-like layers with an average interlayer distance of ~0.37 nm, which is much larger than the kinetic diameter of He (0.26 nm). In previous studies on He diffusion in silica glass, the He atoms that diffused into the voids of silica glass make the glass significantly less compressible at high pressures.[23,24] This substantial change in the compressibility was revealed by the nearly unchanged first sharp diffraction peak (FSDP) position of SiO_2 glass in a He medium under pressures up to 18.6 GPa. By analogy, if He diffused into GC through the spaces between the graphene-like layers, it would make the interlayer spacing seemingly incompressible. To investigate this, we conducted in situ high-pressure XRD experiments on GC using He as a pressure medium.

Figure 2a shows the XRD patterns of GC at representative different pressures in the presence of He. The FSDP, whose position corresponds to the interlayer distance of the graphene-like layers, shows a clear shift toward higher two-theta angles with increasing pressure. The position of the FSDP as a function of pressure was determined by fitting the peak to a Gaussian function (see Figure 2b). For comparison, we included results from previous studies that used Ne as a pressure medium and from experiments conducted without any pressure medium.[16,27] The consistent results from all three independent experiments suggest that the compression behavior of GC has not been affected by the presence of pressure mediums He or Ne. The minor differences among different studies primarily arise from experimental uncertainties in determining the peak positions, given the weak and broad nature of the FSDP. If He were intercalating between the graphene-like layers of GC, it would make the interlayer spacing highly incompressible and result in a stable FSDP position, similar to what is observed in silica.[23,24] Therefore, these XRD results indicate that He does not likely diffuse into GC through the interlayer spaces, despite the interlayer distance of 0.37 nm being larger than the kinetic diameter of He (0.26 nm). Moreover, since He has the smallest kinetic diameter among all volatiles, these results further suggest that other volatiles are also unlikely to diffuse into GC through the interlayer spaces under similar conditions.

As previously mentioned, six-membered carbon rings in graphene are nearly impermeable to all gases and liquids, including He.[25] Thus, it is unlikely for He to diffuse through the six-membered rings in GC. On the other hand, previous studies on graphene have shown that gas transport can occur through angstrom-sized pores in graphene when the pore size is comparable to the kinetic diameter of the gas.[32,33] Therefore, it is plausible that gases diffuse through defects or voids within the graphene-like fragments of GC, or along the edges of these fragments, where the atomic structure is more disordered and exhibits lower atomic density, conditions that favor gas diffusion. In crystalline materials, defects such as grain boundaries and dislocations often serve as fast diffusion pathways, with diffusivities at defect cores several orders of magnitude higher than in the perfect lattice.[34,35] Our results suggest that the diffusivity in amorphous materials is also not uniform and that substantial short-circuit diffusion may also occur in amorphous materials, which is consistent with structural and dynamic heterogeneity in amorphous materials revealed by other techniques.[36,37]

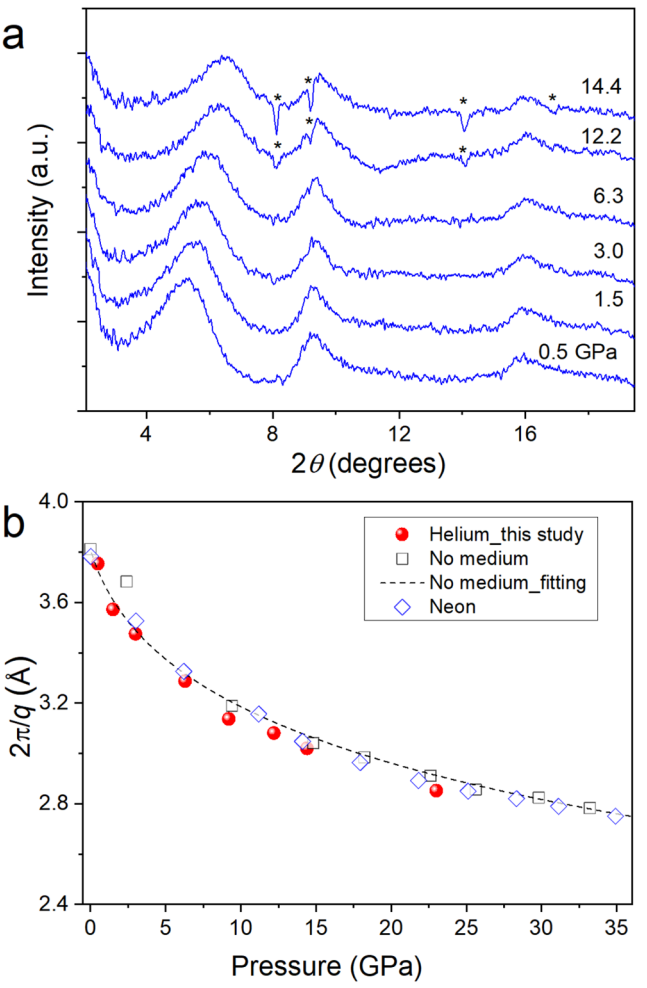

Figure 2. (a) XRD patterns of GC at different pressures during compression with He as the pressure-transmitting medium in a DAC. Due to the weak X-ray scattering ability of GC, the sample XRD patterns are obtained after subtracting the background scattering. The symbol * denotes the peaks from the gasket Re in the background XRD patterns. (b) Position of FSDP as a function of pressure (red circle). The peak position was converted to $2\pi/q$ for easier comparison with previous results. The position of FSDP derived from previous experiments using Ne as a pressure medium (diamond) and without pressure medium (square) are also included for comparison.[16,27]

Since gas diffusion in GC does not rely on its unique graphene-like layered structure but instead most likely proceeds via a defect-mediated mechanism, pressure-induced permeability may be a universal feature of disordered carbon. To test this hypothesis, we need to conduct high-pressure experiments on other forms of sp^2-bonded carbon with disordered atomic structures and abundant enclosed pores or voids. To this end, amorphous hollow carbon nanospheres, combined with Ar as the pressure medium, serve as an ideal model system due to their well-defined pore structures and strong SAXS contrast. Figure 3a shows the TEM image of the carbon nanospheres used in the experiments, revealing their hollow structure with an average size of approximately 60 nm. The highly diffused diffraction rings in the electron diffraction image (Figure 3b) indicate that these nanospheres are

https://doi.org/10.1021/jacs.5c17051
J. Am. Chem. Soc. XXXX, XXX, XXX−XXX

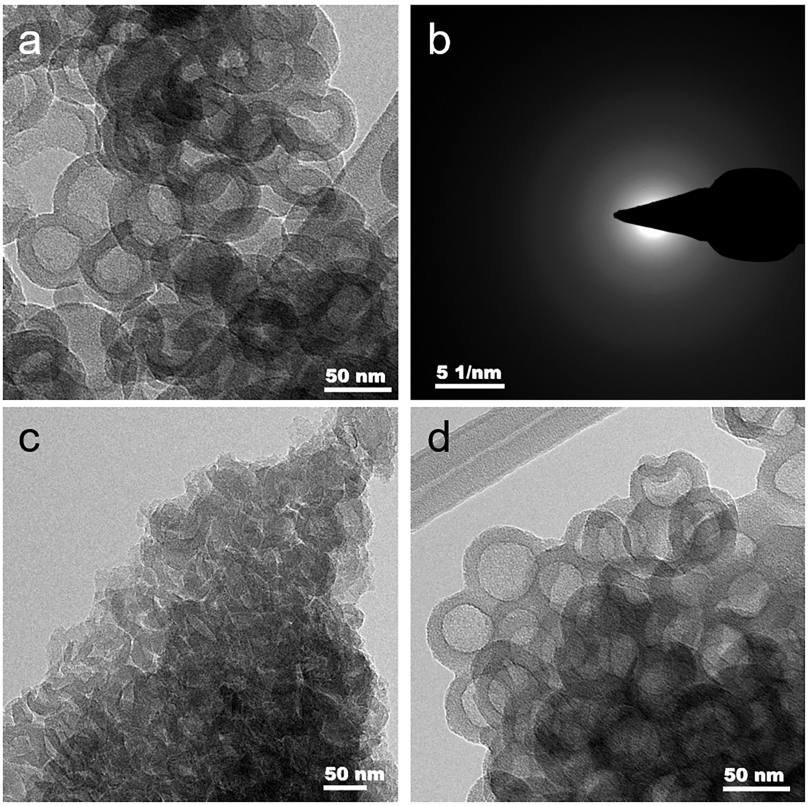

Figure 3. TEM characterization of initial and high-pressure recovered hollow carbon nanosphere samples. (a) TEM image of hollow carbon nanospheres with an average outer diameter of ∼60 nm. (b) Electron diffraction image of the carbon nanospheres showing highly diffused diffraction rings. (c) TEM image of hollow carbon nanospheres after compression to ∼20 GPa without a pressure medium, followed by decompression. (d) TEM image of hollow carbon nanospheres recovered from ∼20 GPa with Ar as the pressure medium.

amorphous. Given their hollow structure, if Ar diffuses into the carbon nanospheres under pressure, then it would fill the empty cores of the nanospheres, altering their compression behavior. Figure 3c,d shows the TEM images of the carbon nanosphere sample after decompression from ∼20 GPa without a pressure medium or with an Ar pressure medium, respectively. In Figure 3c, most hollow structures appear to be destroyed by compression, which is expected, as the empty core structure of nanospheres would collapse under high pressure, similar to the squashing observed in carbon nanotubes.[38] In contrast, the hollow structures remain largely intact in Figure 3d, which can be attributed only to the diffusion of Ar into the cores of the nanospheres, supporting their shells during compression and preventing their collapse.

To further quantitatively verify Ar diffusion and assess its generality in hollow amorphous carbon nanospheres under pressure, we performed in situ high-pressure SAXS experiments on an additional batch of amorphous carbon nanospheres with different sizes. Figures 4a, b and S2 and S3 display the TEM and high-resolution TEM images of these nanospheres, indicating an average outer diameter of ∼200 nm and a disordered atomic structure quite different from GC. High-pressure SAXS was used to investigate the permeability of the nanospheres to Ar. As shown in Figure 4c, the SAXS pattern at ambient pressure shows a distinct hump at 0.02−0.03 $Å^{-1}$ and a weaker one at ∼0.05 $Å^{-1}$ (indicated by vertical arrows), which can be attributed to the density contrast between the amorphous carbon shell and the empty cores. After loading Ar to 0.3 GPa, the hump at 0.02 to 0.03 $Å^{-1}$ becomes significantly weaker, and the one at ∼0.05 $Å^{-1}$ nearly disappears.

The experimental data were fitted using Irena software to interpret the SAXS results (see Figures 4d and S4).[28] A core−shell form factor was employed to model the scattering signal from the hollow carbon nanospheres (see the Supporting Information for detailed fitting information). To fit the SAXS profiles at 0 and 0.3 GPa, a similar size distribution for the carbon nanospheres was used, while the contrast (scattering length density difference $\Delta\rho$) between the shell and core/surrounding medium was adjusted. The fitting results indicate that $\Delta\rho$ between the shell and the core decreases by ∼70% at 0.3 GPa. This dramatic change suggests that Ar has diffused into the empty cores of the carbon nanospheres, reducing the core−shell scattering contrast ($\Delta\rho^2$) by over 90%. Therefore, the SAXS results suggest that Ar can effectively diffuse into the amorphous carbon nanospheres, even at relatively low pressures, such as 0.3 GPa. It should be noted that the size of nanospheres only slightly decreases when compressed to 0.3 GPa, which is minimal and can be neglected for data fitting. For instance, previous studies suggest the volumes of type I and type II GC decrease by ∼5% (corresponding to a size decrease of 1.7%) when compressed to 0.5−1 GPa.[31]

It should be noted that the 0 GPa SAXS data for both GC and amorphous hollow carbon nanospheres were collected after decompression rather than before gas loading. Due to the impermeability of both GC and amorphous carbon under ambient conditions, a small amount of residual gases should remain trapped in their nanopores after decompression. The influence of this residual gas has been evaluated in our previous study, in which SAXS data of a GC sample were collected before compression, compressed to 0.3 GPa (with Ar as the

https://doi.org/10.1021/jacs.5c17051
J. Am. Chem. Soc. XXXX, XXX, XXX−XXX

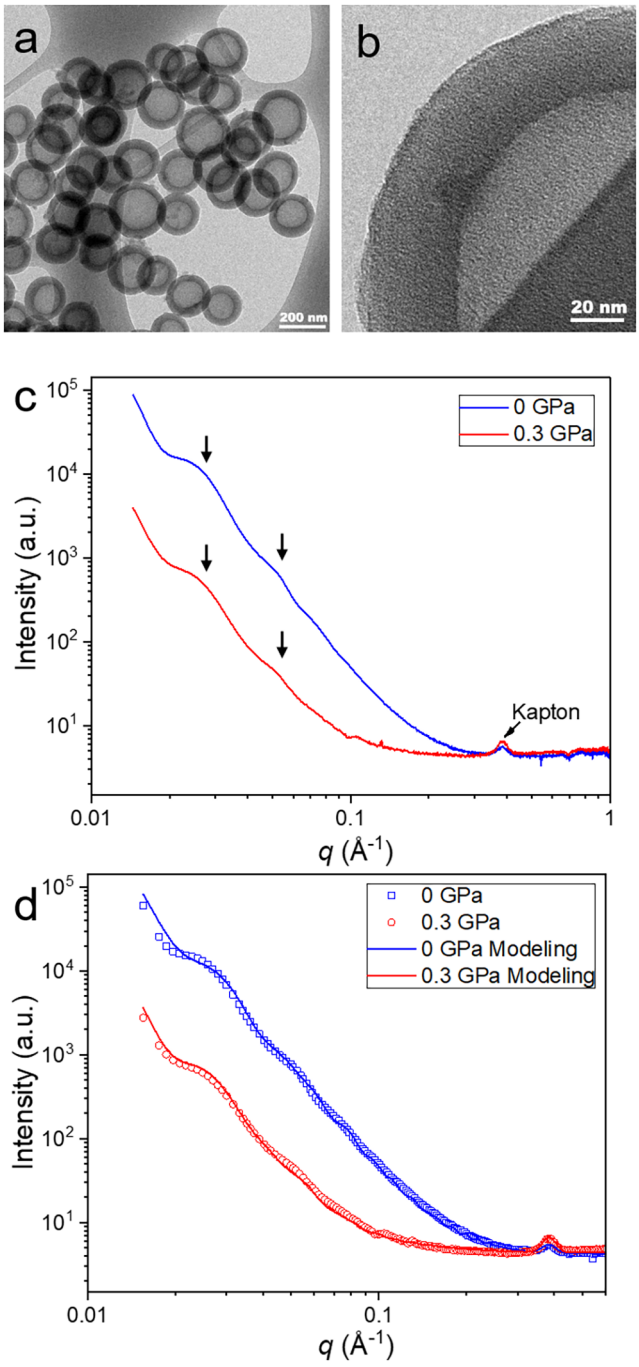

Figure 4. In situ high-pressure SAXS of hollow carbon nanospheres (a). TEM image of hollow carbon nanospheres with an average outer diameter of ∼200 nm. (b). High-resolution TEM image of a hollow carbon nanosphere showing the disordered atomic structure. (c). SAXS curves of hollow carbon nanospheres in a DAC at 0.3 GPa with Ar as the pressure-transmitting medium (red curve) and at 0 GPa (blue curve) after decompression. The peak at ∼0.4 $Å^{-1}$ originates from the Kapton foil used as the window material for the vacuum tube in which the SAXS detector is placed. (d) Comparison of experimental data (circles and squares) and the fitting results (solid lines).

pressure medium), and again after full decompression.[11] As shown in Figure S5, the pressure of residual Ar trapped in the nanopores after decompression to 0 GPa is much lower than the pressure needed to significantly modify the SAXS contrast and does not measurably affect the signal from the pore structure. Therefore, the 0 GPa data collected after decompression could still represent the initial pore structure, which justifies the simplified experimental protocol adopted in the present work.

The observation that Ar penetrates these nanospheres at modest pressures supports the generality of pressure-induced defect-mediated diffusion in disordered sp^2-bonded carbon. Since Ar has a relatively large kinetic diameter (0.35 nm), our results imply that other gases with smaller kinetic diameters (e.g., Ne: 0.28 nm, He: 0.26 nm) could also effectively diffuse into these amorphous carbon nanospheres under pressure. With good gas permeability under pressure, these nanospheres and various other amorphous carbon with similar structures could serve as promising candidates for synthesizing NDCs. From a microstructural perspective, the amorphous carbon with numerous enclosed pores would be particularly suitable for this purpose, as these pores can act as high-pressure sample chambers. Amorphous carbon materials can be synthesized using various methods, and their microstructures are highly tunable, ranging from hollow nanospheres investigated in this study to monolayers, nanoporous, mesoporous structures, etc.[39,40] These versatile characteristics make these amorphous carbon materials good candidates for NDC synthesis precursors.

CONCLUSIONS

In this study, the pressure-induced diffusion of He and Ar into GC and amorphous carbon nanospheres was systematically investigated by multiple techniques, including in situ high-pressure XRD, high-pressure SAXS, and TEM. It is revealed that He does not diffuse into GC through the interlayer spacing between the graphene-like layers but rather through disordered structural defects. Further experiments indicate that, in addition to GC, amorphous carbon hollow nanospheres can also efficiently take up gases under moderate pressures (<0.3 GPa), suggesting that they can serve as viable precursors for NDC synthesis as well (preliminary tests and finite-element modeling indicate that the ratio between the shell thickness and hollow size is a key parameter governing their ability to retain high internal pressures). These results suggest that pressure-induced permeability is a general phenomenon in disordered carbon structures, not limited to GC, and highlight a promising route for designing tunable carbon precursors for future NDC synthesis. Overall, this work deepens our fundamental understanding of volatile diffusion in carbon materials in general and provides essential insights into the development of synthesizing strategies of NDCs, thereby promoting preservation of high-pressure volatiles for diverse applications, including the potential development of ambient condition solid deuterium−tritium fuel target capsules (with a hollow carbon structure) for inertial confinement fusion.

ASSOCIATED CONTENT

Supporting Information

The Supporting Information is available free of charge at https://pubs.acs.org/doi/10.1021/jacs.5c17051.

Experimental methods; TEM characterization of the hollow carbon nanospheres with an average outer diameter of ∼200 nm; and a comparison of experimental SAXS data of GC and carbon nanospheres with modeling results (PDF)

https://doi.org/10.1021/jacs.5c17051
J. Am. Chem. Soc. XXXX, XXX, XXX−XXX

AUTHOR INFORMATION

Corresponding Authors

Zhidan Zeng − *Center for High Pressure Science and Technology Advanced Research (HPSTAR), Shanghai 201203, China;* orcid.org/0000-0003-4283-2393; Email: zengzd@hpstar.ac.cn

Qiaoshi Zeng − *Center for High Pressure Science and Technology Advanced Research (HPSTAR), Shanghai 201203, China; Shanghai Key Laboratory of Material Frontiers Research in Extreme Environments (MFree), Shanghai Advanced Research in Physical Sciences (SHARPS), Shanghai 201203, China;* orcid.org/0000-0001-5960-1378; Email: zengqs@hpstar.ac.cn

Authors

Hongbo Lou − *Center for High Pressure Science and Technology Advanced Research (HPSTAR), Shanghai 201203, China; Shanghai Key Laboratory of Material Frontiers Research in Extreme Environments (MFree), Shanghai Advanced Research in Physical Sciences (SHARPS), Shanghai 201203, China*

Fujun Lan − *Center for High Pressure Science and Technology Advanced Research (HPSTAR), Shanghai 201203, China; Shanghai Key Laboratory of Material Frontiers Research in Extreme Environments (MFree), Shanghai Advanced Research in Physical Sciences (SHARPS), Shanghai 201203, China; Shanghai Institute of Laser Plasma, Shanghai 201800, China*

Xiao Sun − *Deutsches Elektronen-Synchrotron DESY, Hamburg 22607, Germany;* orcid.org/0000-0001-5428-3526

Yuxin Liu − *Center for High Pressure Science and Technology Advanced Research (HPSTAR), Shanghai 201203, China*

Hongwei Sheng − *Department of Physics and Astronomy, George Mason University, Fairfax, Virginia 22030-4444, United States*

Ho-kwang Mao − *Center for High Pressure Science and Technology Advanced Research (HPSTAR), Shanghai 201203, China; Shanghai Key Laboratory of Material Frontiers Research in Extreme Environments (MFree), Shanghai Advanced Research in Physical Sciences (SHARPS), Shanghai 201203, China*

Complete contact information is available at: https://pubs.acs.org/10.1021/jacs.5c17051

Author Contributions

[#]Z.Z. and H.L. contributed equally to this work.

Notes

The authors declare no competing financial interest.

ACKNOWLEDGMENTS

The authors acknowledge the financial support from the National Natural Science Foundation of China (Grant No. 12574001), Shanghai Science and Technology Committee, China (No. 22JC1410300), and the Shanghai Key Laboratory of Material Frontiers Research in Extreme Environments, China (No. 22dz2260800). Parts of this research were carried out at beamline P62 of PETRA-III, DESY, and the beamtime was allocated for proposal I-20220926. Parts of this research were carried out at BL40XU of SPring-8 (proposal No. 2023A1073). The authors thank the Shanghai Synchrotron Radiation Facility of BL15U1 (https://cstr.cn/31124.02.SSRF.BL15U1) and 16B1 (https://cstr.cn/31124.02.SSRF.BL16B1) for the assistance on XRD and SAXS measurements. Portions of this work were performed at GeoSoilEnviroCARS (the University of Chicago, Sector 13) and beamline 12-ID-B, Advanced Photon Source (APS), Argonne National Laboratory. GeoSoilEnviroCARS was supported by the National Science Foundation − Earth Sciences (EAR-1634415). This research used resources of the Advanced Photon Source, a U.S. Department of Energy (DOE) Office of Science User Facility operated for the DOE Office of Science by Argonne National Laboratory under Contract No. DE-AC02-06CH11357.

REFERENCES

(1) Drozdov, A. P.; Eremets, M. I.; Troyan, I. A.; Ksenofontov, V.; Shylin, S. I. Conventional superconductivity at 203 K at high pressures in the sulfur hydride system. *Nature* **2015**, *525*, 73−76.

(2) Eremets, M. I.; Drozdov, A. P.; Kong, P. P.; Wang, H. Semimetallic molecular hydrogen at pressure above 350 GPa. *Nat. Phys.* **2019**, *15* (12), 1246−1249.

(3) Ji, C.; Adeleke, A. A.; Yang, L.; Wan, B.; Gou, H.; Yao, Y.; Li, B.; Meng, Y.; Smith, J. S.; Prakapenka, V. B.; Liu, W.; Shen, G.; Mao, W. L.; Mao, H.-k. Nitrogen in black phosphorus structure. *Sci. Adv.* **2020**, *6* (23), No. eaba9206.

(4) Laniel, D.; Winkler, B.; Fedotenko, T.; Pakhomova, A.; Chariton, S.; Milman, V.; Prakapenka, V.; Dubrovinsky, L.; Dubrovinskaia, N. High-Pressure Polymeric Nitrogen Allotrope with the Black Phosphorus Structure. *Phys. Rev. Lett.* **2020**, *124* (21), No. 216001.

(5) Loubeyre, P.; Occelli, F.; Dumas, P. Synchrotron infrared spectroscopic evidence of the probable transition to metal hydrogen. *Nature* **2020**, *577* (7792), 631−635.

(6) Somayazulu, M.; Dera, P.; Goncharov, A. F.; Gramsch, S. A.; Liermann, P.; Yang, W.; Liu, Z.; Mao, H.-k.; Hemley, R. J. Pressure-induced bonding and compound formation in xenon−hydrogen solids. *Nat. Chem.* **2010**, *2* (1), 50−53.

(7) Spaulding, D. K.; Weck, G.; Loubeyre, P.; Datchi, F.; Dumas, P.; Hanfland, M. Pressure-induced chemistry in a nitrogen-hydrogen host−guest structure. *Nat. Commun.* **2014**, *5* (1), No. 5739.

(8) Hou, J.; Wang, X.; Zhu, Q.; Shao, X.; Qiu, S.; Weng, X.-J.; Yang, G.; Dong, X.; Zhou, X.-F.; Tian, Y. Chemical Bonding between Helium and Fluorine under Pressure. *J. Am. Chem. Soc.* **2025**, *147*, 33453−33459.

(9) Sun, L.; Banhart, F.; Krasheninnikov, A. V.; Rodríguez-Manzo, J. A.; Terrones, M.; Ajayan, P. M. Carbon Nanotubes as High-Pressure Cylinders and Nanoextruders. *Science* **2006**, *312* (5777), 1199−1202.

(10) Mao, H.-K.; Mao, W. L. Geomimicry—-Liberating high-pressure research by encapsulation. *Matter Radiat. Extremes* **2022**, *7* (6), No. 068102.

(11) Zeng, Z.; Wen, J.; Lou, H.; Zhang, X.; Yang, L.; Tan, L.; Cheng, B.; Zuo, X.; Yang, W.; Mao, W. L.; Mao, H.-k.; Zeng, Q. Preservation of high-pressure volatiles in nanostructured diamond capsules. *Nature* **2022**, *608* (7923), 513−517.

(12) Liang, T.; Zeng, Z.; Yang, Z.; Lan, F.; Lou, H.; Yang, C.; Peng, D.; Liu, Y.; Luo, T.; Xing, Z.; Wang, Q.; Ke, H.; Yang, Y.; Che, R.; Sheng, H.; Mao, H.-k.; Zeng, Q. Preserving high-pressure solids via freestanding thin-film engineering. *Nat. Commun.* **2025**, *16* (1), No. 5777.

(13) Harris, P. J. F. Fullerene-related structure of commercial glassy carbons. *Philos. Mag.* **2004**, *84* (29), 3159−3167.

(14) Shiell, T. B.; Wong, S.; Yang, W.; Tanner, C. A.; Haberl, B.; Elliman, R. G.; McKenzie, D. R.; McCulloch, D. G.; Bradby, J. E. The composition, structure and properties of four different glassy carbons. *J. Non Cryst. Solids* **2019**, *522*, No. 119561.

(15) Vieira, L. d. S. A review on the use of glassy carbon in advanced technological applications. *Carbon* **2022**, *186*, 282−302.

(16) Lin, Y.; Zhang, L.; Mao, H.-k.; Chow, P.; Xiao, Y.; Baldini, M.; Shu, J.; Mao, W. L. Amorphous Diamond: A High-Pressure Superhard Carbon Allotrope. *Phys. Rev. Lett.* **2011**, *107* (17), No. 175504.

(17) Hu, M.; He, J.; Zhao, Z.; Strobel, T. A.; Hu, W.; Yu, D.; Sun, H.; Liu, L.; Li, Z.; Ma, M.; Kono, Y.; Shu, J.; Mao, H.-k.; Fei, Y.; Shen, G.; Wang, Y.; Juhl, S. J.; Huang, J. Y.; Liu, Z.; Xu, B.; Tian, Y. Compressed glassy carbon: An ultrastrong and elastic interpenetrating graphene network. *Sci. Adv.* **2017**, *3* (6), No. e1603213.
(18) Yao, M.; Fan, X.; Zhang, W.; Bao, Y.; Liu, R.; Sundqvist, B.; Liu, B. Uniaxial-stress-driven transformation in cold compressed glassy carbon. *Appl. Phys. Lett.* **2017**, *111* (10), No. 101901.
(19) Zeng, Z.; Yang, L.; Zeng, Q.; Lou, H.; Sheng, H.; Wen, J.; Miller, D. J.; Meng, Y.; Yang, W.; Mao, W. L.; Mao, H.-k. Synthesis of quenchable amorphous diamond. *Nat. Commun.* **2017**, *8* (1), No. 322.
(20) Li, Z.; Wang, Y.; Ma, M.; Ma, H.; Hu, W.; Zhang, X.; Zhuge, Z.; Zhang, S.; Luo, K.; Gao, Y.; Sun, L.; Soldatov, A. V.; Wu, Y.; Liu, B.; Li, B.; Ying, P.; Zhang, Y.; Xu, B.; He, J.; Yu, D.; Liu, Z.; Zhao, Z.; Yue, Y.; Tian, Y.; Li, X. Ultrastrong conductive in situ composite composed of nanodiamond incoherently embedded in disordered multilayer graphene. *Nat. Mater.* **2023**, *22*, 42−49.
(21) Huang, X.; Shiell, T. B.; Salek, A.; Aghajamali, A.; Suarez-Martinez, I.; Sun, Q.; Strobel, T. A.; McKenzie, D. R.; Marks, N. A.; McCulloch, D. G.; Bradby, J. E. Comparison of hydrostatic and non-hydrostatic compression of glassy carbon to 80 GPa. *Carbon* **2024**, *219*, No. 118763.
(22) Rothwell, W. S. Small-Angle X-Ray Scattering from Glassy Carbon. *J. Appl. Phys.* **1968**, *39* (3), 1840−1845.
(23) Sato, T.; Funamori, N.; Yagi, T. Helium penetrates into silica glass and reduces its compressibility. *Nat. Commun.* **2011**, *2* (1), No. 345.
(24) Shen, G.; Mei, Q.; Prakapenka, V.; Lazor, P.; Sinogeikin, S.; Meng, Y.; Park, C. Effect of helium on structure and compression behavior of SiO2 glass. *Proc. Natl. Acad. Sci. U.S.A.* **2011**, *108*, 6004−6007.
(25) Sun, P. Z.; Yang, Q.; Kuang, W. J.; Stebunov, Y. V.; Xiong, W. Q.; Yu, J.; Nair, R. R.; Katsnelson, M. I.; Yuan, S. J.; Grigorieva, I. V.; Lozada-Hidalgo, M.; Wang, F. C.; Geim, A. K. Limits on gas impermeability of graphene. *Nature* **2020**, *579* (7798), 229−232.
(26) Bunch, J. S.; Verbridge, S. S.; Alden, J. S.; van der Zande, A. M.; Parpia, J. M.; Craighead, H. G.; McEuen, P. L. Impermeable Atomic Membranes from Graphene Sheets. *Nano Lett.* **2008**, *8* (8), 2458−2462.
(27) Zeng, Z.; Sheng, H.; Yang, L.; Lou, H.; Tan, L.; Prakapenka, V. B.; Greenberg, E.; Zeng, Q. Structural transition in cold-compressed glassy carbon. *Phys. Rev. Mater.* **2019**, *3* (3), No. 033608.
(28) Ilavsky, J.; Jemian, P. R. Irena: tool suite for modeling and analysis of small-angle scattering. *J. Appl. Crystallogr.* **2009**, *42* (2), 347−353.
(29) Wang, S.; Meng, Y. F.; Ando, N.; Tate, M.; Krasnicki, S.; Yan, C. S.; Liang, Q.; Lai, J.; Mao, H. K.; Gruner, S. M.; Hemley, R. J. Single-crystal CVD diamonds as small-angle X-ray scattering windows for high-pressure research. *J. Appl. Crystallogr.* **2012**, *45* (Pt 3), 453−457.
(30) Fujisawa, T. High Pressure Small-Angle X-Ray Scattering. In *High Pressure Bioscience: Basic Concepts, Applications and Frontiers*; Akasaka, K.; Matsuki, H., Eds.; Springer Netherlands: Dordrecht, 2015; pp 663−675.
(31) Zhao, Z.; Wang, E. F.; Yan, H.; Kono, Y.; Wen, B.; Bai, L.; Shi, F.; Zhang, J.; Kenney-Benson, C.; Park, C.; Wang, Y.; Shen, G. Nanoarchitectured materials composed of fullerene-like spheroids and disordered graphene layers with tunable mechanical properties. *Nat. Commun.* **2015**, *6*, No. 6212.
(32) Wang, L.; Drahushuk, L. W.; Cantley, L.; Koenig, S. P.; Liu, X.; Pellegrino, J.; Strano, M. S.; Scott Bunch, J. Molecular valves for controlling gas phase transport made from discrete ångström-sized pores in graphene. *Nat. Nanotechnol.* **2015**, *10* (9), 785−790.
(33) Sun, P. Z.; Yagmurcukardes, M.; Zhang, R.; Kuang, W. J.; Lozada-Hidalgo, M.; Liu, B. L.; Cheng, H. M.; Wang, F. C.; Peeters, F. M.; Grigorieva, I. V.; Geim, A. K. Exponentially selective molecular sieving through angstrom pores. *Nat. Commun.* **2021**, *12* (1), No. 7170.
(34) Chesser, I.; Koju, R. K.; Mishin, Y. Atomic-level mechanisms of short-circuit diffusion in materials. *Int. J. Mater. Res.* **2024**, *115* (2), 85−105.
(35) Mishin, Y.; Herzig, C. Grain boundary diffusion: recent progress and future research. *Mater. Sci. Eng.: A* **1999**, *260* (1), 55−71.
(36) Ichitsubo, T.; Matsubara, E.; Yamamoto, T.; Chen, H. S.; Nishiyama, N.; Saida, J.; Anazawa, K. Microstructure of Fragile Metallic Glasses Inferred from Ultrasound-Accelerated Crystallization in Pd-Based Metallic Glasses. *Phys. Rev. Lett.* **2005**, *95* (24), No. 245501.
(37) Qiao, J. C.; Wang, Q.; Pelletier, J. M.; Kato, H.; Casalini, R.; Crespo, D.; Pineda, E.; Yao, Y.; Yang, Y. Structural heterogeneities and mechanical behavior of amorphous alloys. *Prog. Mater. Sci.* **2019**, *104*, 250−329.
(38) Chen, C.; Lin, Y.; Zhou, W.; Gong, M.; He, Z.; Shi, F.; Li, X.; Wu, J. Z.; Lam, K. T.; Wang, J. N.; Yang, F.; Zeng, Q.; Guo, J.; Gao, W.; Zuo, J.-M.; Liu, J.; Hong, G.; Antaris, A. L.; Lin, M.-C.; Mao, W. L.; Dai, H. Sub-10-nm graphene nanoribbons with atomically smooth edges from squashed carbon nanotubes. *Nat. Electron.* **2021**, *4* (9), 653−663.
(39) Toh, C.-T.; Zhang, H.; Lin, J.; Mayorov, A. S.; Wang, Y.-P.; Orofeo, C. M.; Ferry, D. B.; Andersen, H.; Kakenov, N.; Guo, Z.; Abidi, I. H.; Sims, H.; Suenaga, K.; Pantelides, S. T.; Özyilmaz, B. Synthesis and properties of free-standing monolayer amorphous carbon. *Nature* **2020**, *577* (7789), 199−203.
(40) Lu, P.; Sun, Y.; Xiang, H.; Liang, X.; Yu, Y. 3D Amorphous Carbon with Controlled Porous and Disordered Structures as a High-Rate Anode Material for Sodium-Ion Batteries. *Adv. Energy Mater.* **2018**, *8* (8), No. 1702434.

https://doi.org/10.1021/jacs.5c17051
J. Am. Chem. Soc. XXXX, XXX, XXX−XXX